Available online at www.sciencedirect.com

ScienceDirect

Energy Procedia 114 (2017) 3140 – 3149

Energy Procedia

13th International Conference on Greenhouse Gas Control Technologies, GHGT-13, 14-18 November 2016, Lausanne, Switzerland

Innovation achieved in geomechanics research in the BIGCCS centre

Pierre Cerasi[a] *, Alexandre Lavrov[a], Anna Stroisz[a], Jørn Stenebråten[a], Robert Cuss[b], Andrew Wiseall[b], Jon Harrington[b], Caroline Graham[b] and David Noy[b]

[a]*SINTEF Petroleum Research, Formation Physics dept, PB 4760 Sluppen, 7465 Trondheim, Norway*
[b]*British Geological Survey, Environmental Science Centre Keyworth, Nottingham, NG12 5GG, UK*

Abstract

As part of the BIGCCS centre in Trondheim, Norway, a task in the sub-project dealing with CO_2 sequestration looked at geomechanics and its significance for successful storage planning and operation. Innovation in this domain includes a laboratory activity, at SINTEF Petroleum Research, for examining thermal stress related fracturing risk in shale caprock and to test bonding strength between cement and rock by use of composite cement/rock plugs, whereas at BGS in Nottingham, UK, a bespoke shear rig to study permeability of faults as a function of stress history.

Peer-review under responsibility of the organizing committee of GHGT-13.

Keywords: Geomechanics; cement; shale; fault; shear; strength; wettability.

---

1. Introduction

The BIGCCS Centre for environmentally friendly energy research has been in operation in Trondheim, Norway, for the past eight years. BIGCCS encompassed all aspects of the CCS chain and was administered by SINTEF Energy, while the sub-project dedicated to storage was administered by SINTEF Petroleum Research. In this sub-project a dedicated task was established to look at geomechanics, rock physics, and related aspects of caprock sealing. An add-on project obtained fresh funding from the Research Council of Norway for the years 2012-2014; the project title was:

---

* Corresponding author. Tel.: +47-993-409-28.
E-mail address: pierre.cerasi@sintef.no

Peer-review under responsibility of the organizing committee of GHGT-13.
doi:10.1016/j.egypro.2017.03.1442

"Fundamental Effects of CO_2 on Rock Properties". This paper describes central innovative ideas and methods developed within the framework of this project. In addition, an innovation made at the British Geological Survey (BGS) related to geomechanical activity in the framework of BGS's participation in BIGCCS, is included here as well.

When injecting CO_2 from ships, it is expected that temperature contrasts may arise between the injection well and the near-well surroundings [1]. The latter include the metal casing and cement sheath completing the well, plus the different formations to which the well cement bonds. A new methodology was developed whereby simple tests can establish the temperature difference beyond which tensile fracture occurs due to the sole effect of thermal stress build-up [2].

A second new laboratory method was developed, this time to probe the mechanical properties of the interface between rock and cement. The developed method should provide the input required for geomechanical simulations looking at debonding risk assessment in injection wells, as a function of local stress evolution. The method consists in preparing composite plugs, half cement and half rock, under controlled stress and temperature conditions [3]. The obtained composite plugs were then tested in compression and direct tension modes. By making several plugs with varying interface angle relative to the plug axis, it is possible to evaluate the interface strength and the friction angle.

The third innovation reported here pertains to BGS's construction of a rig to investigate conditions for reactivation of faults [4]. Injection of CO_2 results in a change of the stress-state in the underground. An increase in pore pressure can be high enough to trigger reactivation of faults, potentially causing leakage or damage to infrastructure. The overall aim of the rig is thus to explore the operational limits for safe injection, by shearing typical fault gouge and measure changes in its hydraulic conductivity.

2. Thermal stress measurement in the laboratory

Fracturing could occur in the near-well area if large enough thermal stresses arise in situations with strong temperature contrasts between the injected CO_2 and the formations on the outside of the well casing and cement sheath. Such risk would typically arise in cases where cold liquid CO_2 is injected while friction down the well is not sufficient to heat it, thus maintaining a large temperature difference along the well. This scenario would be likely for offshore injection, directly from ships, carrying the CO_2 in liquid state and where heating prior to injection would not be sufficient to avoid cooling of the formations around the well. The sealing rock immediately above the injection reservoir is most often some variant of shale formation. The temperature contrast between the injected CO_2 (or for that matter any other liquid) and the shale formation, for which tensile fracturing occurs due to the development of tensile stresses exceeding the rock's tensile strength, was modelled numerically [5]. These tensile, thermal stresses will occur if the rock is not able to deform to respond to the temperature changes.

In the laboratory, however, it is difficult to reproduce the same conditions in a traditional load frame for compression testing with axial pistons. Maintaining the pistons in a fixed position while cooling the cylindrical rock specimen inserted in the load frame, would lead to the plug detaching from the top piston instead of fracturing, unless strongly glued to the pistons.

A practical solution to this problem was found by reversing the situation from cooling to heating, thus making the specimen expand instead of contracting. Compression stress developing in such a situation (where the frame pistons would be kept immobile) can be made to initiate transverse tensile stress in the middle of the specimen, provided that the specimen geometry be a disk and the pistons modified such that only a line contact is achieved with the specimen. This geometry is commonly advocated for the standard indirect tensile test for rocks, the so-called Brazilian test.

A new variant of the Brazilian test was developed at SINTEF, whereby thermally-induced tensile fracturing can be studied experimentally, by performing a test where the rock is subjected to mechanical pre-loading and subsequent heating, taking care to heat only the rock, not the metal frame parts (Fig. 1). The developed method uses powerful spot heating of the rock with infra-red light, while maintaining constant piston position.

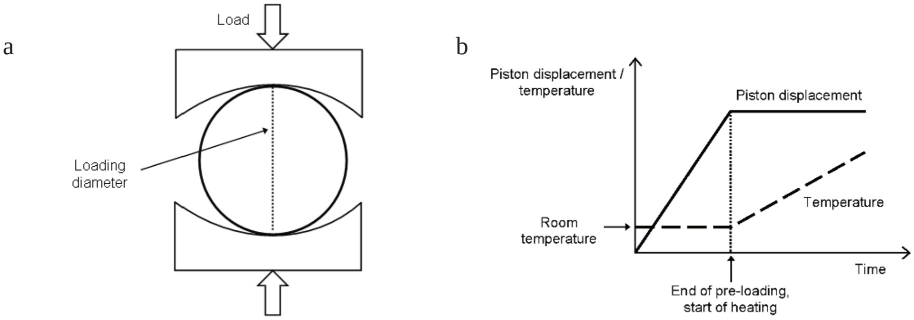

Fig. 1. (a) Schematic illustration of conventional Brazilian test; (b) loading and heating schedules in thermal Brazilian test.

A verification experiment was conducted with Mancos shale; the disk had a diameter of 48 mm and a thickness of 24 mm. The specimen was pre-loaded to 5 kN along its diameter on an MTS uniaxial compression load frame. The loading diameter was parallel to the bedding planes. Care was taken not to fracture the specimen during pre-loading. Pre-loading was performed with constant displacement rate. After the target pre-load value of 5 kN had been reached, the piston position was fixed, and the specimen underwent some (unintended) stress relaxation. Heating of the two flat faces of the disc was then carried out using two infrared lamps (Fig. 2a). Thermocouples were used to measure the temperature at one of the flat faces of the disc and on the adjacent metal piston; the readings from the piston thermocouple showed negligible increase in temperature.

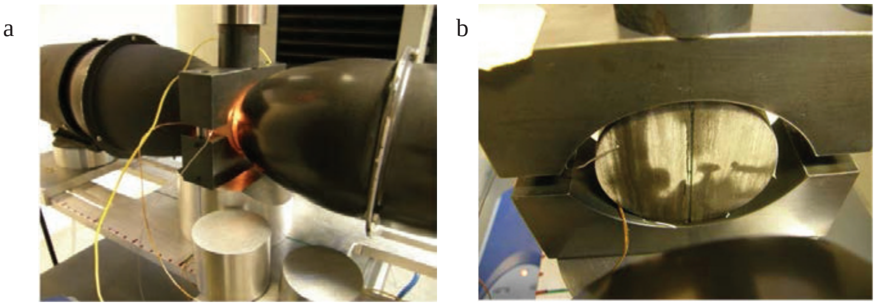

Fig. 2. (a) Experimental setup with infrared lamps; (b) Specimen of Mancos shale with thermally induced tensile diametrical fracture.

The timelines of the measured temperature at one of the flat faces and the indirect tensile stress in the center of the disc, calculated from the monitored load values, are shown in Fig. 3. Heating eventually resulted in the formation of a tensile fracture (Fig. 2b), at 1800 s in Fig. 3. Failure was observed as a sharp drop in the load. The failure mode was typical of Brazilian tests performed with the loading diameter parallel to bedding, i.e. a fracture running parallel to the loading diameter (Fig. 2b).

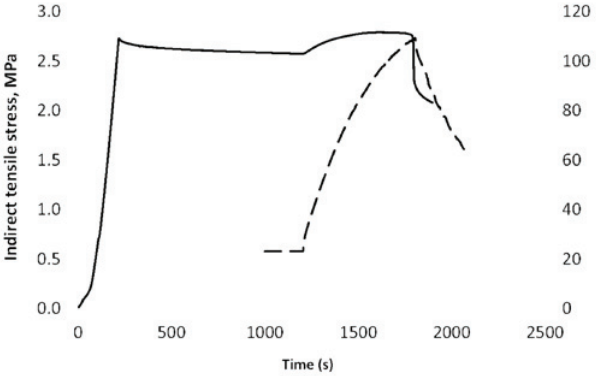

Fig. 3. Plot of temperature (dashed line) measured on a flat face of Mancos shale disc, and stress evolution (solid line) in thermal Brazilian test.

2.1. Discussion, conclusions and further work

The proof-of-concept study presented above has demonstrated the viability of the thermal Brazilian test as a tool for investigation of tensile fracturing in rocks caused by thermal tensile stresses. The specific details of the test, i.e. the pre-load level, the heating rate, the maximum applied temperature, must be chosen in accord with thermal and mechanical properties of the rock. Infrared lamps provide a satisfactory heating source in the thermal Brazilian test. The thermal Brazilian test is thus a promising new method for studying thermally-induced tensile fracturing in rocks (and other materials). An unexpected outcome from the experiment was the large increase in temperature required to create a modest increase in axial load. Should this be verified for shale cores from considered storage sites, this would point to a negligible risk of thermal fracturing as a leakage initiation mechanism through primary sealing shale barriers.

Further work should address the effect of bedding orientation on severity of thermal stress development, heating rate effect on integrity of sample and investigation of creep propensity by allowing for longer hold periods at a given temperature.

3. Fundamental exploration of cement-to-rock bonding

Previous work at SINTEF has focused on cement bond shear strength measurement, using the punch-out method on hollow cylinder rock plugs with the borehole filled with cement [6]. This, as part of systematic studies to quantify the risk of leakage in the immediate neighborhood of CO_2 injection wells. The studies looked at multiple micro-annulus creation scenarios, where debonding may occur between casing and cement or between cement and rock, with various interface conditions, such as drilling fluid film or filter cake remains [7].

A new method was devised, to look at fundamental measurement of failure under compression and tension of a relatively smooth cement-to-rock interface. The objective was to provide much needed input data for numerical modelling, where shear strength, friction angle, failure angle and not least the tensile strength of the cement bond are vital parameters. These parameters can then be used to simulate realistic downhole stress path scenarios and help quantify conditions leading to leakage path formation as a function of lithology and cement type and rock formation.

The mechanical loading tests were designed so as to either shear the cement interface under various normal loads or expose the interface to tensile stresses under direct tension loading. A load frame was used to test the cement interface under uniaxial compression or direct tension mode. For the compression tests, cylindrical Berea sandstone plugs, of

1.5" diameter, were used with an inclined saw cut made to prepare a surface on which cement was made to bond. These planar surfaces were cut at different angles with respect to the plug's axis. Portland class G cement was then poured in a heat shrink sleeve, on the top of the pre-cut rock in order to reconstitute a cylindrical plug. The rock/cement mixture was then placed in a metal pre-compaction casing under 20 MPa uniaxial stress and 60 °C for 24h to 72h (Fig. 4). Plugs created in this manner were kept in an oven for further curing at 60 °C over several days.

For the direct tension tests, plugs were prepared in a similar manner as above, only that the interface was prepared with a surface angle of 0° with respect to the plug's axis (that is, parallel to the end surfaces of the composite plug). Tests were then run in uniaxial tension mode (Fig. 5).

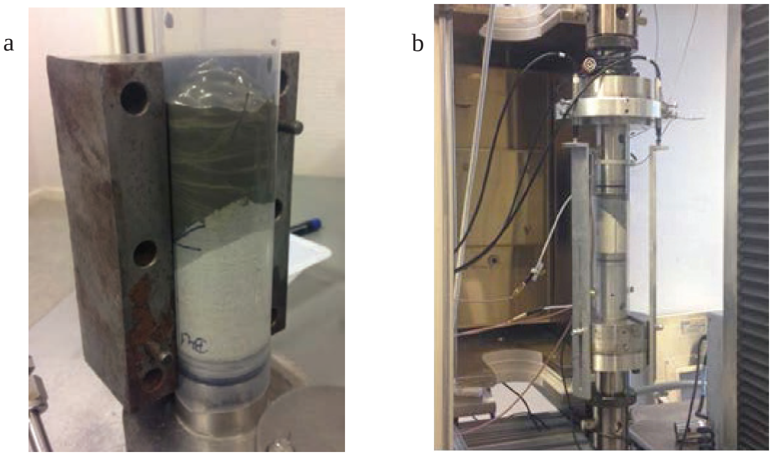

Fig. 4. (a) Preparation of composite plugs of cement and Berea sandstone under uniaxial compaction; (b) uniaxial load frame with computer-controlled steering system. A composite plug is inserted in the load frame.

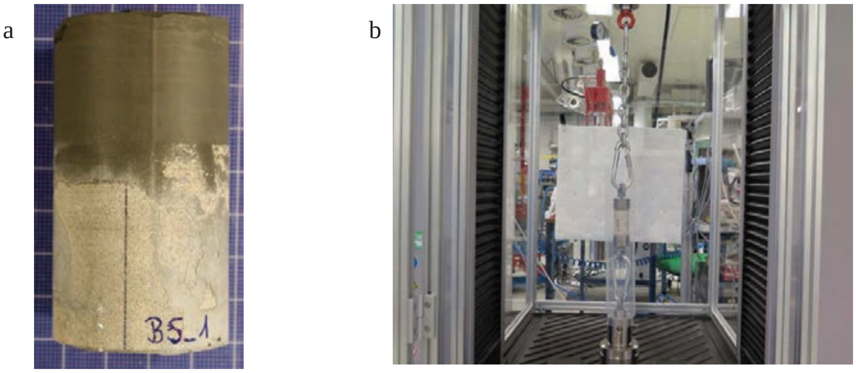

Fig. 5. (a) Composite plug with interface perpendicularly oriented to the plug axis; (b) uniaxial load frame set-up for direct tensile strength testing.

3.1. Results

Both uniaxial compression tests and direct tension tests indicate that the strongest location in the composite plug actually is the interface between the two materials. This is at least true for cement hardening on permeable sandstone under drained oedometer stress conditions. Failure always occurred, in our tests, inside the sandstone part of the plug, suggesting that both the cured cement and its interface with the sandstone were significantly stronger (Fig. 6). This was also reflected by the values of compressive and tensile strength, in agreement with those measured for the Berea sandstone used in these plugs, i.e. 80 MPa and 2 MPa, respectively.

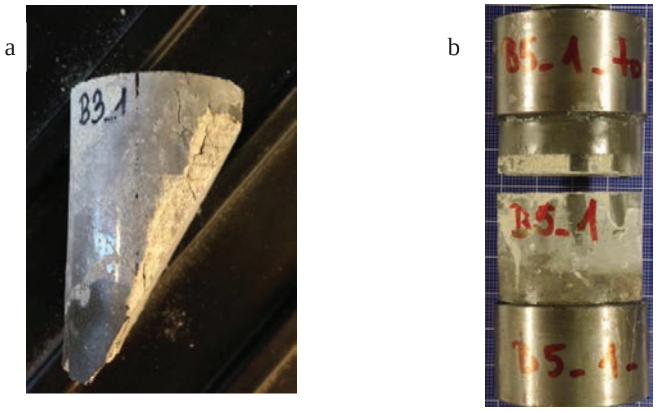

Fig. 6. Failure of composite plugs inside the sandstone part: (a) compressive shear failure; (b) tensile failure.

In order to investigate the effect of pore pressure in the sandstone on the interface strength, additional direct tensile tests were carried out. The plugs were saturated with 3.5 wt% NaCl brine and the pore pressure brought up to 5 MPa. Maintaining the pore pressure constant, cement was again poured on top of the half-plug (cut perpendicular to its axis) in the oedometric cell. The cement was subjected to 20 MPa axial stress at 60 °C, as in the previous test series. The plug was then tested again in direct tension, by removing the oedometer cell and reversing the piston movement so as to pull on the plug's end face, glued with epoxy to a metal cup (as in Fig. 6). The tensile strength was measured as 1.3 MPa. As previously, failure occurred in the sandstone, but in one case closer to, and touching the interface (Fig. 7).

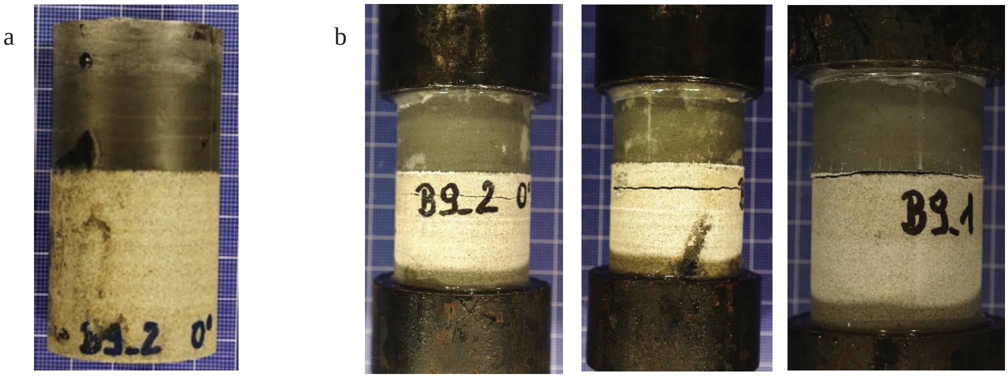

Fig. 7. Tensile test of composite plug prepared with 5 MPa pore pressure in the sandstone: (a) intact plug; (b) tensile failure in the sandstone and near the interface.

3.2. Conclusion and further work

A new method was devised to measure the mechanical properties of the cement to rock interface, in order to provide input for numerical models of near-well integrity. The interface was considered, as early indications pointed to it being the weakest link in cement bonded to rock. However, previous studies had not subjected the cement to high compression as expected immediately above an injection interval. The results from the initial tests presented above point towards the interface being the strongest link, contrary to expectations. Failure occurred in both cases in the sandstone, for the tensile tests, although in one of the tests with hardening of cement on top of sandstone with 5 MPa pore pressure, the fracture was much closer to the interface, touching it in part of the circumference. A small difference was recorded in the tensile strength of the plugs, 2 MPa for dry sandstone vs. 1.3 MPa for the saturated plug. This difference may be either due to sensitivity of the sandstone to brine, in terms of dissolution of clay cement, or natural variability between the different plugs tested. Since the compression tests did not produce clean shearing of the interface, it can only be concluded here that the shear strength of the interface is above that of the sandstone.

Further work should address composite plugs made of shale and cement, as the chemical interaction between the two while the cement hardens may affect the resulting interface strength. Also, repeat tests with sandstone should explore higher pore pressure values in the sandstone and mud contamination on the sandstone face prior to cementing.

4. Bespoke shear rig for fault reactivation studies

Fault reactivation occurs when the rock on both sides of the fault slip, resulting most times in dilation of the low permeability gouge core, thereby increasing hydraulic conductivity of the fault. This will happen upon sufficient increase in the pore pressure, on one side of the fault, for example following injection of CO_2.

The stress-state in the vicinity of the fault and its evolution after injection is started can be plotted in the stress space, as shown in Fig. 8. When pore pressure is sufficient, the Mohr circle of the faults of orientation θ may touch the failure envelope, signifying stress conditions that could cause reactivation.

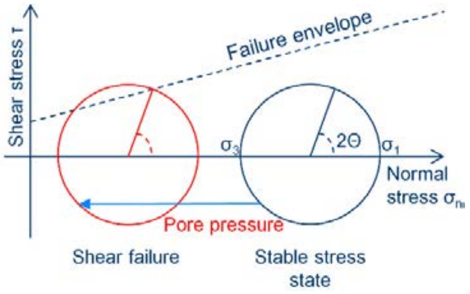

Fig. 8. Mohr stress-state circles with Coulomb shear failure envelope. The red circle represents the altered effective stresses upon increase in pore pressure. If the red circle contacts the failure envelope, shear slippage occurs on the fault, provided it is oriented at the corresponding angle to the principal stresses.

However, this representation may be an over-simplification of reality; indeed, it does not consider the fault gouge mineralogy, the state of the injected fluid, or complex stress histories. Thus, an experimental rig was constructed with the aim to explore the operational limits for safe injection. The apparatus is a shear device in which fault gouge is placed between top and bottom blocks (Fig. 9) and compressed with vertical load up to 12 MPa. Variable shear rate can be applied to the gouge, with rates varying between 1 mm per 2 secs all the way down to 1 mm per 3 months. The top block has dimensions 60 × 60 mm; an injection port through it allows for injection pressure between 0.5 MPa to 22

MPa. Ensuing fracture thickness is recorded by two eddy-current sensors with sub-micron accuracy; the vertical displacement is also measured to sub-micron accuracy. The pore pressure can be measured at 2 locations on the fracture plane. For the gouge, tests were conducted with Kaolinite paste and Ball Clay paste.

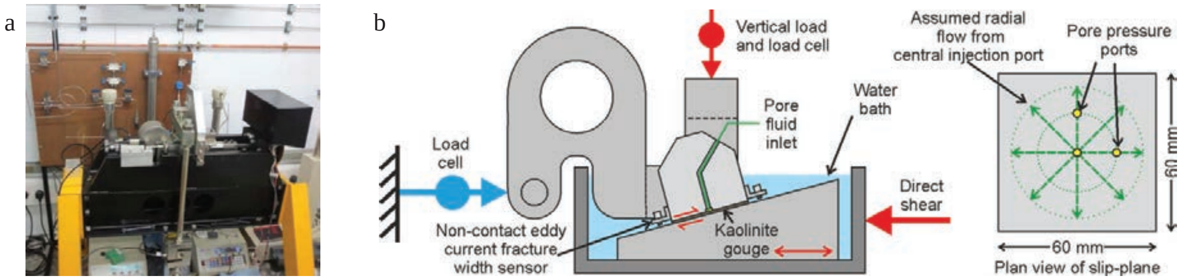

Fig. 9. Bespoke shear rig at BGS: (a) photograph of the assembled rig; (b) schematic cross and plan views.

4.1. Results

A total of 33 tests have been conducted so far. Each shear test was conducted over 24 hours, showing good repeatability for the mechanical response. Such tests provide the initial shear stress, the shear modulus, the yield stress and the peak stress (Fig. 10). A linear relationship was seen for initial shear stress, yield and peak stress, as a function of applied vertical stress (Fig. 11). Fault reactivation is identified in this set-up by a change in vertical displacement and shear stress. Some tests show single slip events, while others show multiple events. Collecting the test results, fault reactivation failure envelopes could be plotted. A single envelope was obtained when plotting the results in *q-p'* space (Fig. 12).

Only one of seven gas injection tests resulted in fault reactivation. Fault reactivation with gas injection did not occur at low pressures when pore pressure exceeded the reactivation pressure seen for water.

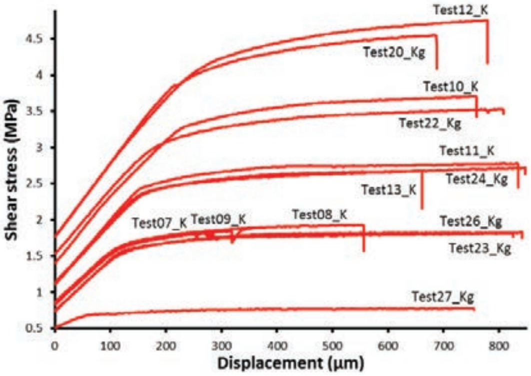

Fig. 10. Shear tests conducted on new BGS shear rig.

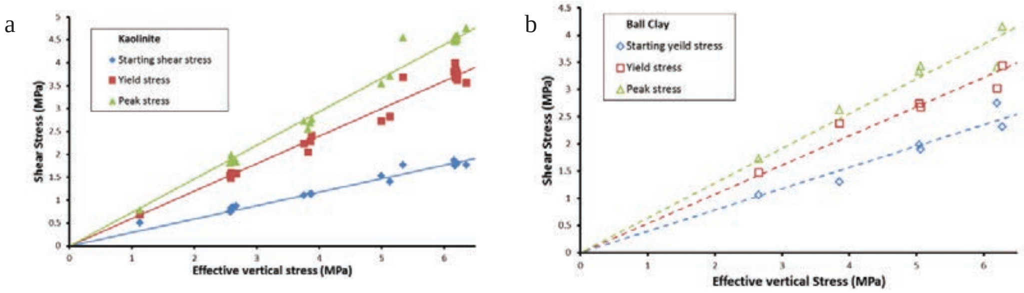

Fig. 11. Linear relationship between applied vertical effective stress and initial, yield and peak shear stress: (a) for Kaolinite; (b) for Ball Clay.

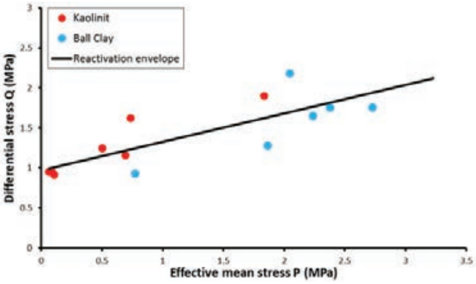

Fig. 12. Failure envelope in Q-P space (axial – vertical stress as a function of effective mean stress).

4.2. Conclusion and further work

The new state-of-the-art shear rig has been able to show that fault reactivation during fluid injection occurs when pressure exceeds the yield stress for Kaolinite gouge and is only marginally above the starting shear stress for Ball Clay. Fault reactivation has proven to be difficult to achieve for gaseous injection as the clay fabric deforms to accommodate a localized elevated pore pressure. This tends to confirm that the stress space representation of fault reactivation with Mohr circles is an over-simplification.

Further work will include higher vertical stresses and a range of additional gouge compositions to better understand the effect of mineralogy on fault reactivation. It is also anticipated that the saturation state of the gouge and the fracture roughness will play a role, which requires further experimentation.

4. General conclusion

Among the various activities dedicated to geomechanics in the BIGGCS centre, the three topics presented here led to innovations thought to help accelerate CCS. All three are laboratory methodologies targeting the identified areas in a CO_2 storage operation with highest geomechanical risk. These are namely the near-well area with highest risk of leakage around injection wells and reservoir compartment-bounding faults. In the near-well area, cement bonding to formation rocks is obviously critical in order to eliminate seepage upwards along the well path. Such seepage may short-circuit the sealing formations located above the storage reservoir. Being able to gather the mechanical properties needed for numerical simulations will help increasing confidence in such simulations when looking at the effect of possible stress paths on wellbore integrity. Similarly, looking at the formation itself, just outside the injection wells is critical in order to plan the most cost-effective injection strategy. This implies minimal pre-heating of the CO_2 to be injected and therefore requires confidence in the injection not jeopardizing integrity by causing large thermal tensile stresses to arise in the sealing caprock. Farther afield, bounding faults have long been recognized as a major threat to CO_2 containment in its intended sequestration compartment. However, faults have so far been represented in coupled geomechanical models as simple 2D surfaces obeying simplified Mohr-Coulomb or similar failure laws. The tool developed by BGS will help the geomechanics community gain better understanding of the complexities of fault behavior, in terms of response to stress hysteresis, activation differences with different fluids and pore pressure development as well as taking into account the effect of the gouge material properties on global response of the fault.

As such, all three innovations can provide simple tools for the authorities and storage site developers to systematically quantify the risk associated with planned operations from the geomechanical viewpoint. This may be further developed to suggest guidelines for site approval with recommended allowed values for the properties of cement and formation rocks in terms of safe temperature contrasts, injection rates, etc.

Acknowledgements

This publication has been produced with support from the BIGCCS Centre, performed under the Norwegian research program Centres for Environment-friendly Energy Research (FME). The authors acknowledge the following partners for their contributions: Gassco, Shell, Statoil, TOTAL, GDF SUEZ and the Research Council of Norway (193816/S60).

References

[1] Krogh E, Nilsen R, Henningsen R. Liquefied CO_2 injection modelling. Energy Procedia 23 (2012) 527–555.

[2] Cerasi P, Stroisz A, Walle LE, Lavrov A (2014). Laboratory testing of shale rock specimens to assess thermal fracturing risk in caprock surrounding injection wells. Paper ARMA 14-7077, 48th US Rock Mechanics / Geomechanics Symposium Proceedings, American Rock Mechanics Association (ARMA), Minneapolis, MN, USA, 1-4 June 2014.

[3] Cerasi P, Stroisz A (2015). Fundamental exploration of cement to rock bonding. Paper ARMA 15-237, 49th US Rock Mechanics / Geomechanics Symposium Proceedings, American Rock Mechanics Association (ARMA), San Francisco, CA, USA, 28 June- 1 July 2015.

[4] Cuss R, Harrington JF (2016). An experimental study of the potential for fault reactivation during changes in gas and pore-water pressure. International Journal of Greenhouse Gas Control, 53. 41-55. 10.1016/j.ijggc.2016.07.028.

[5] Lavrov A, Cerasi P. Numerical modeling of tensile thermal stresses in rock around a cased well caused by injection of a cold fluid (2013). Paper ARMA 13-306, 47th US Rock Mechanics / Geomechanics Symposium Proceedings, American Rock Mechanics Association (ARMA). p. 8.

[6] Opedal N, Todorovic J, Torsæter M, Vrålstad T, Mushtaq W (2014). Experimental Study on the Cement-Formation Bonding. SPE 168138-MS, SPE International Symposium and Exhibition on Formation Damage Control held in Lafayette, Louisiana, USA, 26–28 February 2014.

[7] Opedal N, Torsæter M, Vrålstad T, Cerasi P (2014). Potential Leakage Paths along Cement-formation Interfaces in Wellbores; Implications for CO_2 Storage. Energy Procedia, Volume 51, 2014, Pages 56-64, ISSN 1876-6102, http://dx.doi.org/10.1016/j.egypro.2014.07.007.